Establishing the Range of Applicability of Hydrodynamics in High-Energy Collisions

Victor E. Ambruş,[1] S. Schlichting,[2] and C. Werthmann[2,3,*]
[1]Department of Physics, West University of Timişoara, Bulevardul Vasile Pârvan 4, Timişoara 300223, Romania
[2]Fakultät für Physik, Universität Bielefeld, D-33615 Bielefeld, Germany
[3]Incubator of Scientific Excellence-Centre for Simulations of Superdense Fluids, University of Wrocław, pl. Maxa Borna 9, 50-204 Wrocław, Poland

(Received 16 December 2022; revised 17 February 2023; accepted 7 March 2023; published 14 April 2023)

We simulate the space-time dynamics of high-energy collisions based on a microscopic kinetic description in the conformal relaxation time approximation, in order to determine the range of applicability of an effective description in relativistic viscous hydrodynamics. We find that hydrodynamics provides a quantitatively accurate description of collective flow when the average inverse Reynolds number Re^{-1} is sufficiently small and the early preequilibrium stage is properly accounted for. We further discuss the implications of our findings for the (in)applicability of hydrodynamics in proton-proton, proton-nucleus, and light nucleus collisions.

DOI: 10.1103/PhysRevLett.130.152301

Introduction.—Relativistic heavy ion collisions probe the behavior of strong interaction matter under extreme conditions. One of the central goals of these experiments is to determine the properties of the quark-gluon-plasma (QGP), a new phase of deconfined strongly interacting matter. The emergence of collective phenomena in such collisions has been successfully described using relativistic viscous hydrodynamics [1–6], which in modern simulation frameworks forms the central part of multistage evolution models [7–9].

Despite tremendous phenomenological success, it is important to remember that viscous relativistic hydrodynamics is by construction an effective macroscopic description of the underlying microscopic theory of quantum chromodynamics (QCD), which aims to describe the long-time and long-wavelength behavior of QCD close to equilibrium. Consequently, the applicability of hydrodynamics requires a separation of the timescale and length scale of the dynamics of the microscopic constituents and those of the macroscopic dynamics of the system as a whole as well as some degree of equilibration of the QGP, both of which are not necessarily fulfilled in heavy ion collisions. While for sufficiently high multiplicity events one can expect the system to quickly evolve toward equilibrium, establishing the timescale of this process for practical purposes has so far been mostly guesswork [4]. In recent years, the observation of collective flow phenomena even in small collision systems, that were traditionally considered to be too dilute to allow for QGP formation, has challenged the hydrodynamic paradigm [10–15]. While remarkable progress has been made in understanding the emergence and applicability of hydrodynamic behavior in the simplistic $0+1D$ Bjorken flow [16–31], despite some notable attempts [32–34] the crucial question under what circumstances viscous hydrodynamics provides a reliable and accurate description of the more complex space-time dynamics of real-world collisions remains largely unanswered.

In this Letter, we employ a microscopic description in relativistic kinetic theory to determine the range of applicability of viscous hydrodynamics in high-energy collisions. Starting from a nonequilibrium initial state immediately after the collision, we find that—even in the limit of very large interaction strength—the early time preequilibrium dynamics can never be described by ordinary viscous hydrodynamics which can affect collective flow observables at the few-percent level. Subsequently, for sufficiently large systems, the fluid approaches equilibrium before the onset of the transverse expansion and the development of (anisotropic) transverse flow can nevertheless be described macroscopically using viscous relativistic hydrodynamics. By matching the nonequilibrium kinetic description to relativistic viscous hydrodynamics, we determine a critical inverse Reynolds number Re_c^{-1} below which hydrodynamics can describe the space-time dynamics of the QGP, including the development of anisotropic transverse flow, with a few percent accuracy.

Conversely, for small systems or large viscosity, the system remains out of equilibrium over the course of the evolution and we evaluate when the conditions for the applicability of viscous hydrodynamics are met as a function of shear viscosity to entropy density ratio η/s, initial state energy density, and system size, and thereby infer bounds on the applicability of hydrodynamics in small systems.

Since the reasons for the failure of hydrodynamics at early times can be understood and cured within effectively $0+1D$ Bjorken flow dynamics, we further propose an alternative scheme that allows us to initialize hydrodynamic simulations immediately after the collision $\tau \to 0$ by compensating for the improper description at early times through rescaling the initial conditions.

In this Letter, we focus on the phenomenologically relevant findings and insights noting that our companion paper [35] contains a variety of additional information and details related to our study.

Kinetic theory setup.—In order to study the microscopic evolution of the space-time dynamics, we employ the Boltzmann equation in the relaxation time approximation (RTA),

$$p^\mu \partial_\mu f(x,p) = -\frac{u^\mu(x) p_\mu}{\tau_R(x)}[f(x,p) - f_{\rm eq}(x,p)], \quad (1)$$

with a conformal relaxation time $\tau_R(x) = [(\eta/s)/5T(x)]$. The equilibrium distribution $f_{\rm eq}$ is determined by the temperature $T(x)$ and flow velocity $u^\mu(x)$, which are obtained via Landau matching $u_\mu T^{\mu\nu} = \epsilon u^\nu$, where $\epsilon = aT^4$ denotes the energy density, $a = \nu_{\rm eff}\pi^2/30$ with $\nu_{\rm eff}$ being the effective number of (bosonic) degrees of freedom and $T^{\mu\nu}(x) = \int_p p^\mu p^\nu f(x,p)$ is the energy-momentum tensor (see Ref. [35] for details). Because of the particular simplicity of this microscopic theory, differences in the space-time dynamics of the collision for a fixed initial energy density profile $(\epsilon\tau)_0(\mathbf{x}_\perp)$ only depend on a single dimensionless opacity parameter [33,36]

$$\hat{\gamma} = \frac{1}{5\eta/s}\left(\frac{R}{\pi a}\frac{dE_\perp^0}{d\eta}\right)^{1/4}, \quad (2)$$

which accounts for variations of the shear viscosity to entropy density ratio η/s, as well as of the initial energy per unit rapidity $dE_\perp^0/d\eta = \int_{\mathbf{x}_\perp}(\epsilon\tau)_0(\mathbf{x}_\perp)$ and the system size $R^2 = (dE_\perp^0/d\eta)^{-1}\int_{\mathbf{x}_\perp}\mathbf{x}_\perp^2(\epsilon\tau)_0(\mathbf{x}_\perp)$. In order to have a well-defined collision geometry, we focus on Pb + Pb collision at LHC energies and employ an average initial-state energy density profile $(\epsilon\tau)_0(\mathbf{x}_\perp)$ obtained from a saturation model [37] and vary η/s as well as the centrality of the collision to assess the opacity dependence.

We will quantify the development of anisotropic transverse flow in terms of the elliptic energy flow,

$$\varepsilon_p = \frac{\int_{\mathbf{x}_\perp} T_{xx}(\mathbf{x}_\perp) - T_{yy}(\mathbf{x}_\perp) + 2iT_{xy}(\mathbf{x}_\perp)}{\int_{\mathbf{x}_\perp} T_{xx}(\mathbf{x}_\perp) + T_{yy}(\mathbf{x}_\perp)}, \quad (3)$$

which can be inferred directly from the energy-momentum tensor $T^{\mu\nu}$, and thus eliminates uncertainties related to the hadronization process [38–40]. Microscopic simulations in kinetic theory will be contrasted with the macroscopic description in relativistic hydrodynamics by employing the VHLLE hydro code [41], which provides the evolution in Mueller-Israel-Stewart type second-order viscous hydrodynamics [42,43] with conformal equation of state and transport coefficients matched to the RTA Boltzmann equation (see Ref. [35] for details).

Collective flow and applicability of hydrodynamics.—In order to assess the range of applicability of the

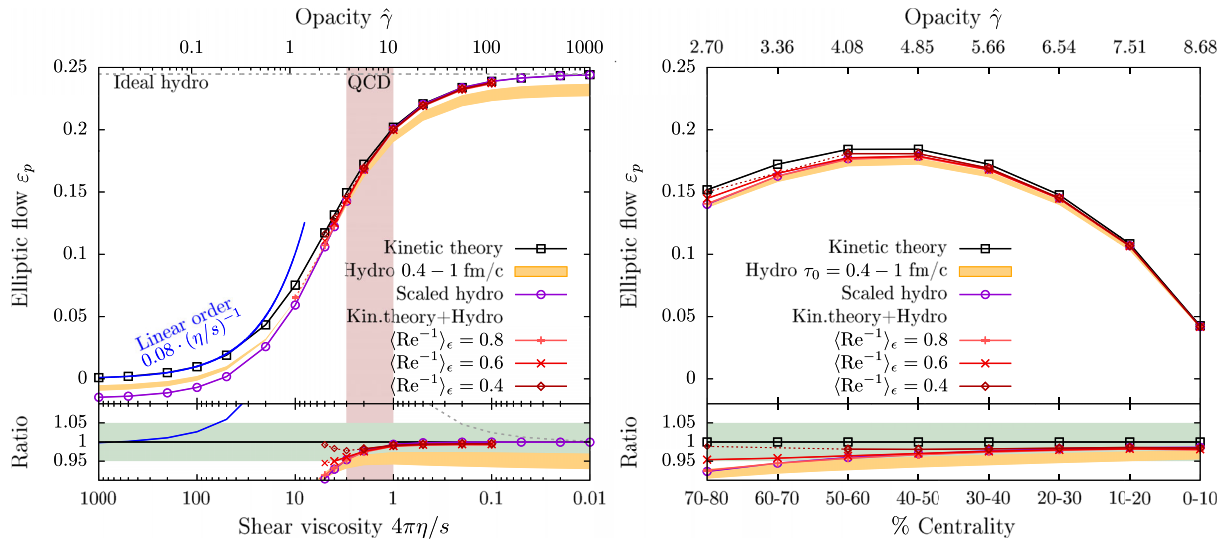

FIG. 1. Variations of the elliptic flow (left) as a function of the shear viscosity to entropy density ratio η/s for 30%–40% Pb + Pb collisions and (right) as a function of collision centrality for fixed $\eta/s = 2/4\pi$. Simulations in kinetic theory (black squares) are compared to ideal (gray dashed) and viscous hydrodynamics (purple circles) as well as hybrid simulations (red pluses, crosses, and diamonds) matching kinetic theory to hydrodynamics at different values of the average inverse Reynolds number Re^{-1}. Bands also show the results for naive hydrodynamics simulations with varying initialization times $\tau_0 = 0.4$–1.0 fm/c. Semianalytic results from a leading order opacity expansion are shown as a blue curve in the left panel.

hydrodynamic description, we compare the results to microscopic simulations in kinetic theory. In Fig. 1 we present the final results [44] (at $\tau = 4R$) for the elliptic energy flow ε_p in 5.02 TeV Pb + Pb collisions as a function of η/s in midcentral collisions (30%–40%) in the left panel and for a realistic value of $\eta/s = 2/4\pi$ as a function of centrality in the right panel. Starting with the results in kinetic theory, one immediately observes a significant opacity dependence of the final state momentum response to the initial state geometry. In the limit of low opacity ($\eta/s \gg 1$), the anisotropic flow is generated by rare final state interactions and can be well described by the leading order opacity expansion [45–51] up to $\hat{\gamma} \lesssim 1$, as indicated by the blue line. Subsequently, for smaller values of η/s the anisotropic flow response increases monotonically as a function of opacity and eventually saturates at large opacities ($\eta/s \ll 1$); it is further interesting to observe that the anticipated values for QCD $4\pi\eta/s \simeq 1$–3 [8,9,52] fall into a regime where the final state response exhibits a significant opacity dependence, where changes of the viscosity η/s by fifty percent result in changes of the anisotropic flow of about 15%.

Now that we have established the baseline from kinetic theory, we can compare the microscopic results to the ones obtained using a hydrodynamic description. Clearly, the first thing to note is that in the limit of infinite opacities ($\eta/s \to 0$), the kinetic theory results converge toward ideal hydrodynamics as indicated by the horizontal line. However, this seemingly obvious agreement is in fact rather nontrivial as we shall explain now. Because of the rapid longitudinal expansion, the system is initially unable to sustain a significant longitudinal pressure, which is only built up over the course of the thermalization process on a timescale $\tau_{\rm eq} \sim \hat{\gamma}^{-4/3}$ [36]. Based on the conformal behavior of the system, this isotropization of the pressure proceeds more rapidly in the hotter regions than in the colder regions of the plasma. Since the system performs work against the longitudinal expansion [23,53], the preequilibrium evolution of the longitudinal pressure affects the evolution of the energy density, resulting in the phenomenon of inhomogeneous longitudinal cooling [36], where hotter regions of the plasma begin to cool faster than colder regions of the plasma, thus leading to a small but non-negligible change of the geometry of the energy density profile even prior to the onset of the (anisotropic) transverse expansion. In contrast, in ideal hydrodynamics the system is always assumed to be in an isotropic local thermal equilibrium state, and the effect of inhomogeneous longitudinal cooling is absent. Hence, in order to restore agreement with ideal hydrodynamics in the limit of infinite opacities ($\eta/s \to 0$), it is in fact necessary to initialize the ideal hydrodynamic simulation with the equilibrated energy density profile (as opposed to the original profile in the limit $\tau \to 0$) as is done in Fig. 1.

While inhomogeneous longitudinal cooling is absent in ideal hydrodynamics, viscous hydrodynamics describes this effect incorrectly as it generically features a negative longitudinal pressure at very early times [24]. Similar to the case of ideal hydrodynamics, this effect can be compensated by a local rescaling of the initial energy density profile. Specifically, we demand that under the 0 + 1-D Bjorken flow evolution, the late-time behavior of the energy density agrees between hydrodynamics and kinetic theory. Mathematically, we make use of the attractor solution for the nonequilibrium evolution of the energy density [23,54]

$$\tau^{4/3}\epsilon = \frac{\tau_0^{4/3}\epsilon_0}{\mathcal{E}(\tilde{w}_0)}\mathcal{E}(\tilde{w}), \tag{4}$$

where $\mathcal{E}$ is a universal function that depends only on the conformal scaling variable $\tilde{w} = \tau T/(4\pi\eta/s)$, with its asymptotic behavior at early and late times given by

$$\mathcal{E}(\tilde{w} \ll 1) = C_\infty^{-1}\tilde{w}^\gamma, \qquad \mathcal{E}(\tilde{w} \gg 1) = 1 - \frac{1}{4\pi\tilde{w}}. \tag{5}$$

Crucially, the coefficients C_∞ and γ that describe the longitudinal cooling at early times take different values in kinetic theory ($\gamma = 4/9, C_\infty^{\rm RTA} \simeq 0.88$) and viscous hydrodynamics [$\gamma = (\sqrt{505} - 13)/18 \simeq 0.526, C_\infty^{\rm hydro} \simeq 0.82$], whereas in ideal hydrodynamics they are trivially determined as $\mathcal{E}(\tilde{w}) = 1, C_\infty = 1$, and $\gamma = 0$. By taking advantage of the fact that in kinetic theory $(\epsilon\tau)_0(\mathbf{x}_\perp)$ is constant at early times, we then initialize the energy density in hydrodynamics as

$$\epsilon_0^{\rm hydro}(\mathbf{x}_\perp) = \left[\left(\frac{4\pi\eta/s}{\tau_0}a^{\frac{1}{4}}\right)^{\frac{1}{2}-\frac{9\gamma}{8}}\left(\frac{C_\infty^{\rm RTA}}{C_\infty^{\rm hydro}}\right)^{9/8}\frac{(\epsilon\tau)_0(\mathbf{x}_\perp)}{\tau_0}\right]^{\frac{8/9}{1-\gamma/4}}. \tag{6}$$

such that upon substituting Eq. (6) into Eq. (4), hydrodynamics and kinetic theory agree at the level of $\tau^{4/3}\epsilon$ when $\tilde{w} \gg 1$ and $\tilde{w}_0 \ll 1$, by virtue of Eq. (5).

By performing such a local rescaling, viscous hydrodynamics can be initialized at arbitrarily early times ($\tau_0 \to 0$) and provides an accurate description of the anisotropic flow down to opacities of $\hat{\gamma} \gtrsim 3$, as can be seen from the purple curve in Fig. 1. We finally note that, if the preequilibrium regime is completely ignored and hydrodynamic simulations are naively initialized with the original energy density profile at a fixed proper time $\tau_0 = 0.4$–1 fm/c, the above effects and the absence of preflow lead to sizable deviations even in the limit of very large opacities. In all cases, similar conclusions can also be reached for the development of radial flow and the cooling of the plasma, as demonstrated explicitly in Supplemental Material [55].

Critical inverse Reynolds number.—Because of the aforementioned subtleties associated with the preequilibrium stage, another viable alternative is to employ a kinetic description at early times when the system is far

from equilibrium and switch to a macroscopic description only once the system is sufficiently close to local thermal equilibrium for hydrodynamics to be applicable. While in phenomenological studies the timescale for initializing hydrodynamic simulations is typically chosen as ~ 1 fm/c [4], a more physical choice can be achieved by monitoring the magnitude of nonequilibrium corrections, as characterized by the (average) inverse Reynolds number [59,62]

$$\mathrm{Re}^{-1} = \left(\frac{6\pi^{\mu\nu}\pi_{\mu\nu}}{\epsilon^2}\right)^{1/2}, \tag{7}$$

where the shear-stress tensor $\pi^{\mu\nu}$ is the nonequilibrium part of $T^{\mu\nu}$. By switching from kinetic theory to hydrodynamics at different values of Re^{-1}, we can then infer what degree of equilibration is required for hydrodynamics to provide an accurate description of the space-time dynamics.

Simulation results for hybrid simulations using kinetic theory + hydrodynamics are also presented in Fig. 1 and are in excellent agreement with the microscopic calculations from kinetic theory at large opacities $\hat{\gamma} \gg 1$. Strikingly, when comparing the results obtained by switching at different $\mathrm{Re}^{-1} = 0.8, 0.6, 0.4$ one observes that the agreement between kinetic theory and hybrid simulations improves significantly with decreasing the inverse Reynolds number at the point of switching. Specifically, when switching at $\mathrm{Re}^{-1} \lesssim 0.75$, the discrepancy between kinetic theory and hybrid simulations remains below 5% irrespective of the viscosity or centrality of the collision. We note, however, that for large viscosities ($4\pi\eta/s \gtrsim 4$) as well as for more peripheral collisions ($\gtrsim$60%), a sufficiently small inverse Reynolds number is only achieved after a long period of evolution in kinetic theory; in order to distinguish this behavior, curves for which the switching time τ/R exceeds the value 0.5 are shown with dashed lines in Fig. 1. Eventually, for very large viscosities $4\pi\eta/s \gtrsim 10$ or very peripheral collisions $\gtrsim$80%, the desired value of Re^{-1} may never be reached throughout the evolution of the system.

Range of applicability of hydrodynamics.—Based on the observation that a critical inverse Reynolds number $\mathrm{Re}_c^{-1} \approx 0.75$ is required for the applicability of viscous hydrodynamics, we can immediately rule out the viability of a hydrodynamic description at small opacities $\hat{\gamma} \lesssim 1$, where the system remains significantly out of equilibrium throughout its entire evolution and this threshold is never reached. However, at smaller viscosities, the aforementioned threshold may be reached very early or at a comparatively late time and the question whether or not hydrodynamics is applicable becomes a more delicate issue. Hence, in order to quantify whether or not hydrodynamics provides a meaningful and accurate description of the space-time dynamics of high-energy collisions, we will compare the timescale τ_{hydro} for the equilibration of the system, determined by requiring $\mathrm{Re}^{-1} < \mathrm{Re}_c^{-1}$, with the onset of the transverse expansion τ_{exp}, determined by requiring that the average transverse flow velocity $\langle u_\perp \rangle_\epsilon$ becomes 0.1 times the speed of light, as depicted in Fig. 2.

Irrespective of the opacity, the transverse expansion sets in on time scales $\tau_{\mathrm{exp}}/R \approx 0.2$ albeit with a slight dependence on the initial energy density profile, as can be seen from the centrality dependence of the curve in the right

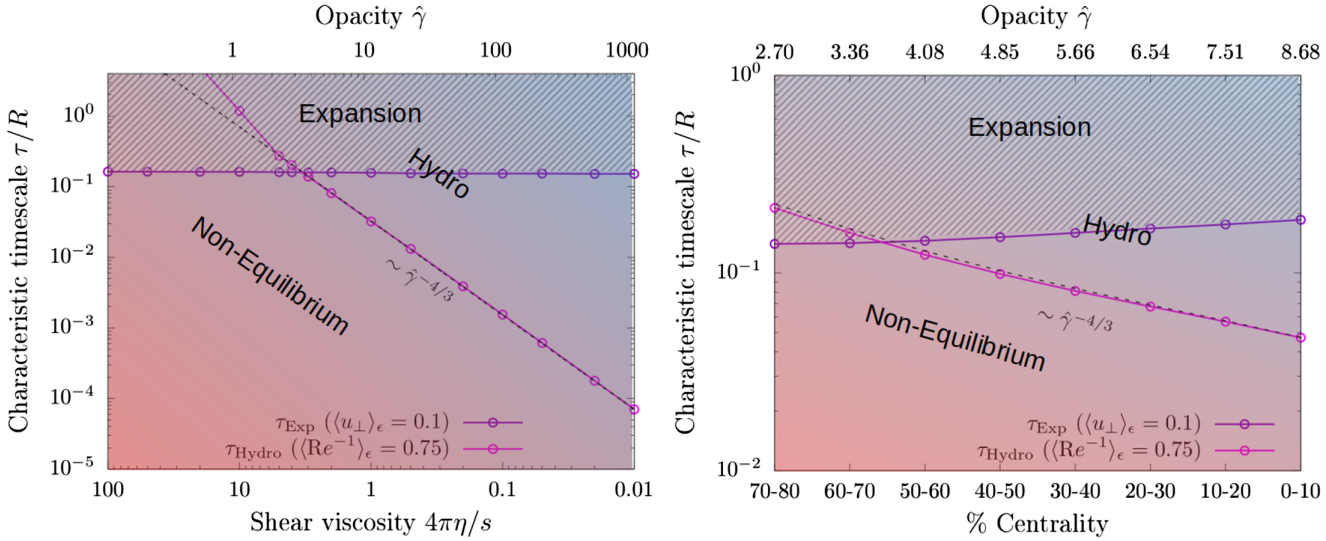

FIG. 2. Characteristic timescales for the onset of the transverse expansion τ_{exp} and the onset of hydrodynamic behavior τ_{hydro} (left) as a function of η/s for 30%–40% Pb + Pb collisions and (right) as a function of collision centrality for fixed $4\pi\eta/s = 2$. Dashed lines indicate the $\hat{\gamma}^{-4/3}$ estimate for the transition between nonequilibrium and hydrodynamic behavior in Eq. (8). Below opacities $\hat{\gamma} \simeq 3$–4, the transverse expansion sets in while the system is significantly out of equilibrium and hydrodynamics is unable to accurately describe the transverse expansion of the system.

panel. Conversely, the timescale for the applicability of hydrodynamics shows a strong opacity dependence [36], which can be quantified semiempirically as [63]

$$\tau_{\rm hydro}/R \approx 1.53\hat{\gamma}^{-4/3}[(\mathrm{Re}_c^{-1})^{-3/2} - 1.21(\mathrm{Re}_c^{-1})^{0.7}], \quad (8)$$

as indicated by the dashed lines in Fig. 2. By comparing the different curves in Fig. 2, one then concludes that for opacities

$$\hat{\gamma} \gtrsim 3\text{–}4, \quad (9)$$

which in Pb + Pb collisions corresponds to $\eta/s \lesssim 3/4\pi$ for 30%–40% centrality or $\lesssim$60% centrality for $\eta/s = 2/4\pi$, the system undergoes equilibration (well) before the onset of the transverse expansion ($\tau_{\rm hydro} < \tau_{\rm exp}$), such that viscous hydrodynamics provides a meaningful and accurate description of the development of (anisotropic) transverse flow. Conversely, for $\hat{\gamma} \lesssim 3$–4 hydrodynamics is not applicable as the system remains out of equilibrium during the transverse expansion ($\tau_{\rm hydro} > \tau_{\rm exp}$) and a genuine nonequilibrium description is required instead.

Conclusions.—Based on a detailed comparison with the microscopic evolution in kinetic theory, we find that viscous hydrodynamics provides an accurate description of the space time dynamics of high-energy heavy-ion collisions, if and only if the system is sufficiently close to equilibrium, as quantified by an inverse Reynolds number [cf. Eq. (7)] $\mathrm{Re}^{-1} \lesssim 0.75$. Clearly, this is not the case during the very early stages of the collision, where irrespective of the shear viscosity to entropy density ratio (η/s) the system is highly anisotropic and the inhomogeneous longitudinal cooling cannot be properly described within ordinary viscous hydrodynamics. Disregarding this effect leads to percent-level deviations in the development of anisotropic transverse flow even in the limit of very small viscosities. However, for sufficiently small viscosities, this effect can be compensated by an inhomogeneous local rescaling of the initial energy density profile [cf. Eq. (6)], or by employing a hybrid description where the energy momentum tensor after the early kinetic evolution provides the initial conditions for the subsequent hydrodynamic stage. It is also conceivable that improved hydrodynamic theories, such as anisotropic hydrodynamics [64–68], or hybrid schemes based on the core-corona picture [69,70] can further push the limits of applicability by improving the description far from equilibrium, and it will be interesting to investigate this further in the future.

Similarly, in very peripheral collisions or if the shear viscosity of the QGP was significantly larger ($\eta/s \gtrsim 3/4\pi$), the system remains out of equilibrium for a significant part or even all of its space-time evolution, such that, if at all, hydrodynamics only becomes applicable at very late times, when the transverse expansion is already very significant. Based on our analysis, we argued that a meaningful and accurate hydrodynamic description of collective flow can be achieved if the opacity $\hat{\gamma}$ [cf. Eq. (2)] exceeds values of $\approx$3–4.

Since within our simplified kinetic description, the nonequilibrium evolution is governed by the single dimensionless opacity parameter $\hat{\gamma}$, it is tempting to speculate about the consequences of our findings for the theoretical description of small collision systems. Based on experimental measurements of the transverse energy per unit rapidity $dE_\perp/d\eta$ and theoretical estimates of the system size, both of which are detailed in Supplemental Material [55], we can deduce that for a typical value of $\eta/s = 2/4\pi$ hydrodynamics is not applicable in minimum bias $p + p$ collisions at LHC energies where opacities typically take values of $\hat{\gamma} \approx 0.7$. Interestingly, the situation is more subtle in p + Pb collisions where opacities range from $\hat{\gamma} \approx 1.5$ in minimum bias events toward the limits of applicability of hydrodynamics in high-multiplicity events where $\hat{\gamma} \approx 2.7$ can be reached. Unfortunately though, the initial state geometry of p + Pb collisions is at present also poorly constrained [71–73], such that it becomes difficult to disentangle the effects of the geometry from the effects of the flow response. However, the onset of hydrodynamic behavior will also be explored in O + O collisions where at LHC energies the estimated opacities reach from 1.4 in peripheral events and 2.2 in midcentral events all the way to 3.1 in central events. Since, as advertised in [74], the collision geometry in O + O collisions is much better constrained, we therefore expect that such collisions will not only provide a crucial test of the applicability of hydrodynamics in heavy-ion collisions but also penetrate into the exciting regime of nonequilibrium QCD in midcentral and peripheral events.

We thank P. Aasha, N. Borghini, H. Elfner, A. Mazeliauskas, H. Roch, A. Shark, and U. A. Wiedemann for valuable discussions. We also thank S. Busuioc for carefully reading the manuscript. This work is supported by the Deutsche Forschungsgemeinschaft (DFG, German Research Foundation) through the CRC-TR 211 "Strong-interaction matter under extreme conditions"—Project No. 315477589—TRR 211. V. E. A. gratefully acknowledges the support through a grant of the Ministry of Research, Innovation and Digitization, CNCS–UEFISCDI, Project No. PN-III-P1-1.1-TE-2021-1707, within PNCDI III. C. W. was supported by the program Excellence Initiative–Research University of the University of Wrocław of the Ministry of Education and Science. Numerical calculations presented in this work were performed at the Paderborn Center for Parallel Computing (PC2) and the Center for Scientific Computing (CSC) at the Goethe-University of Frankfurt and we gratefully acknowledge their support.

*cwerthmann@physik.uni-bielefeld.de

[1] D. A. Teaney, Viscous hydrodynamics and the quark gluon plasma, in *Quark-Gluon Plasma 4*, edited by R. C. Hwa and

X.-N. Wang (World Scientific Publishing Co., Singapore, 2010), pp. 207–266.
[2] H. Song, S. A. Bass, U. Heinz, T. Hirano, and C. Shen, Phys. Rev. Lett. **106**, 192301 (2011).
[3] C. Gale, S. Jeon, and B. Schenke, Int. J. Mod. Phys. A **28**, 1340011 (2013).
[4] U. Heinz and R. Snellings, Annu. Rev. Nucl. Part. Sci. **63**, 123 (2013).
[5] M. Luzum and H. Petersen, J. Phys. G **41**, 063102 (2014).
[6] S. Jeon and U. Heinz, Int. J. Mod. Phys. E **24**, 1530010 (2015).
[7] J. H. Putschke *et al.*, arXiv:1903.07706.
[8] D. Everett *et al.* (JETSCAPE Collaboration), Phys. Rev. C **103**, 054904 (2021).
[9] G. Nijs, W. van der Schee, U. Gürsoy, and R. Snellings, Phys. Rev. C **103**, 054909 (2021).
[10] B. B. Abelev *et al.* (ALICE Collaboration), Phys. Rev. C **90**, 054901 (2014).
[11] M. Aaboud *et al.* (ATLAS Collaboration), Eur. Phys. J. C **77**, 428 (2017).
[12] A. M. Sirunyan *et al.* (CMS Collaboration), Phys. Rev. Lett. **120**, 092301 (2018).
[13] K. Dusling, W. Li, and B. Schenke, Int. J. Mod. Phys. E **25**, 1630002 (2016).
[14] C. Loizides, Nucl. Phys. **A956**, 200 (2016).
[15] J. L. Nagle and W. A. Zajc, Annu. Rev. Nucl. Part. Sci. **68**, 211 (2018).
[16] J. Berges, K. Boguslavski, S. Schlichting, and R. Venugopalan, Phys. Rev. D **89**, 114007 (2014).
[17] J. Berges, K. Boguslavski, S. Schlichting, and R. Venugopalan, J. High Energy Phys. 05 (2014) 054.
[18] M. P. Heller and M. Spalinski, Phys. Rev. Lett. **115**, 072501 (2015).
[19] M. Spaliński, Phys. Lett. B **776**, 468 (2018).
[20] M. Strickland, J. Noronha, and G. S. Denicol, Phys. Rev. D **97**, 036020 (2018).
[21] M. Strickland, J. High Energy Phys. 12 (2018) 128.
[22] M. Spaliński, Phys. Lett. B **784**, 21 (2018).
[23] G. Giacalone, A. Mazeliauskas, and S. Schlichting, Phys. Rev. Lett. **123**, 262301 (2019).
[24] A. Kurkela, W. van der Schee, U. A. Wiedemann, and B. Wu, Phys. Rev. Lett. **124**, 102301 (2020).
[25] G. S. Denicol and J. Noronha, Phys. Rev. Lett. **124**, 152301 (2020).
[26] D. Almaalol, A. Kurkela, and M. Strickland, Phys. Rev. Lett. **125**, 122302 (2020).
[27] M. P. Heller, R. Jefferson, M. Spaliński, and V. Svensson, Phys. Rev. Lett. **125**, 132301 (2020).
[28] X. Du and S. Schlichting, Phys. Rev. Lett. **127**, 122301 (2021).
[29] J.-P. Blaizot and L. Yan, Phys. Rev. C **104**, 055201 (2021).
[30] C. Chattopadhyay, S. Jaiswal, L. Du, U. Heinz, and S. Pal, Phys. Lett. B **824**, 136820 (2022).
[31] X. Du, M. P. Heller, S. Schlichting, and V. Svensson, Phys. Rev. D **106**, 014016 (2022).
[32] G. S. Denicol, U. W. Heinz, M. Martinez, J. Noronha, and M. Strickland, Phys. Rev. D **90**, 125026 (2014).
[33] A. Kurkela, U. A. Wiedemann, and B. Wu, Eur. Phys. J. C **79**, 965 (2019).
[34] A. Kurkela, S. F. Taghavi, U. A. Wiedemann, and B. Wu, Phys. Lett. B **811**, 135901 (2020).
[35] V. E. Ambrus, S. Schlichting, and C. Werthmann, arXiv:2211.14379.
[36] V. E. Ambruş, S. Schlichting, and C. Werthmann, Phys. Rev. D **105**, 014031 (2022).
[37] N. Borghini, M. Borrell, N. Feld, H. Roch, S. Schlichting, and C. Werthmann, Phys. Rev. C **107**, 034905 (2023).
[38] J. I. Kapusta, Phys. Rev. C **21**, 1301 (1980).
[39] H. Petersen, J. Steinheimer, M. Bleicher, and H. Stocker, J. Phys. G **36**, 055104 (2009).
[40] P. Huovinen and H. Petersen, Eur. Phys. J. A **48**, 171 (2012).
[41] I. Karpenko, P. Huovinen, and M. Bleicher, Comput. Phys. Commun. **185**, 3016 (2014).
[42] I. Müller, Z. Phys. **198**, 329 (1967).
[43] W. Israel and J. M. Stewart, Ann. Phys. (N.Y.) **118**, 341 (1979).
[44] In this Letter, we only present final state observables. Further discussion of the time evolution can be found in our companion paper [35].
[45] H. Heiselberg and A.-M. Levy, Phys. Rev. C **59**, 2716 (1999).
[46] N. Borghini and C. Gombeaud, Eur. Phys. J. C **71**, 1612 (2011).
[47] P. Romatschke, Eur. Phys. J. C **78**, 636 (2018).
[48] A. Kurkela, U. A. Wiedemann, and B. Wu, Phys. Lett. B **783**, 274 (2018).
[49] N. Borghini, S. Feld, and N. Kersting, Eur. Phys. J. C **78**, 832 (2018).
[50] A. Kurkela, A. Mazeliauskas, and R. Törnkvist, J. High Energy Phys. 11 (2021) 216.
[51] B. Bachmann, N. Borghini, N. Feld, and H. Roch, Eur. Phys. J. C **83**, 114 (2023).
[52] J. E. Bernhard, J. S. Moreland, and S. A. Bass, Nat. Phys. **15**, 1113 (2019).
[53] J. D. Bjorken, Phys. Rev. D **27**, 140 (1983).
[54] J. Jankowski, S. Kamata, M. Martinez, and M. Spaliński, Phys. Rev. D **104**, 074012 (2021).
[55] See Supplemental Material at http://link.aps.org/supplemental/10.1103/PhysRevLett.130.152301 for additional results regarding radial flow and plasma cooling, discussion of an initial condition closer to common practice, and a disclosure of how we obtained opacity estimates. This material includes Refs. [56–58].
[56] B. B. Abelev *et al.* (ALICE Collaboration), Phys. Lett. B **727**, 371 (2013).
[57] B. B. Abelev *et al.* (ALICE Collaboration), arXiv:2204.10210.
[58] G. Nijs and W. van der Schee, Phys. Rev. C **106**, 044903 (2022).
[59] Our definition follows the convention of Ref. [60], by which Re^{-1} is the ratio between dissipative and equilibrium terms. Note that this differs from the convention commonly used in nonrelativistic fluid dynamics (also in Ref. [61] for heavy ion collisions), where $\mathrm{Re}^{-1} = \eta/\rho u L$ is the ratio of the kinematic viscosity η/ρ to the typical velocity and length scales of the system. Our normalization factor is conventional and chosen such that $\mathrm{Re}^{-1} = 1$ in the limit $\tau \to 0$, where the energy-momentum tensor in kinetic theory assumes the form $T^{\mu\nu} = \mathrm{diag}(\epsilon, \epsilon/2, \epsilon/2, 0)$.
[60] G. S. Denicol, H. Niemi, E. Molnar, and D. H. Rischke, Phys. Rev. D **85**, 114047 (2012); **91**, 039902(E) (2015).

[61] S. Floerchinger and U. A. Wiedemann, J. High Energy Phys. 11 (2011) 100.
[62] H. Niemi and G. S. Denicol, arXiv:1404.7327.
[63] While the factor $\hat{\gamma}^{-4/3}$ and the proportionality to $(\mathrm{Re}_c^{-1})^{-3/2}$ for $(\mathrm{Re}_c^{-1}) \ll 1$ follow from the properties of the Bjorken flow attractor, the numerical pre-factor and the correction term have been determined from a fit to our simulation results.
[64] M. Martinez and M. Strickland, Nucl. Phys. **A848**, 183 (2010).
[65] W. Florkowski and R. Ryblewski, Phys. Rev. C **83**, 034907 (2011).
[66] W. Florkowski, R. Ryblewski, and M. Strickland, Phys. Rev. C **88**, 024903 (2013).
[67] M. Martinez, R. Ryblewski, and M. Strickland, Phys. Rev. C **85**, 064913 (2012).
[68] M. McNelis, D. Bazow, and U. Heinz, Comput. Phys. Commun. **267**, 108077 (2021).
[69] K. Werner, Phys. Rev. Lett. **98**, 152301 (2007).
[70] Y. Kanakubo, Y. Tachibana, and T. Hirano, Phys. Rev. C **101**, 024912 (2020).
[71] S. Demirci, T. Lappi, and S. Schlichting, Phys. Rev. D **106**, 074025 (2022).
[72] B. Schenke and R. Venugopalan, Phys. Rev. Lett. **113**, 102301 (2014).
[73] H. Mäntysaari, B. Schenke, C. Shen, and W. Zhao, Phys. Lett. B **833**, 137348 (2022).
[74] J. Brewer, A. Mazeliauskas, and W. van der Schee, arXiv:2103.01939.